Evaluation of left ventricular function using cardiac magnetic resonance imaging

Suchi Grover, MBBS,[a,b] Darryl P. Leong, MBBS (Hons), MPH,[a] and Joseph B. Selvanayagam, MBBS (Hons), DPhil[a,b]

ASSESSMENT OF LEFT VENTRICULAR FUNCTION

Non-invasive imaging of the left ventricle plays a vital role in the evaluation of most cardiac disease states. Left ventricular (LV) imaging may permit diagnosis of myocardial, coronary, and valvular pathology; provide prognostic information for patients with known cardiovascular disease; and allow for monitoring of response to therapy. Evaluation of LV function is the cornerstone of initial assessment in patients presenting with any new heart disease. In heart failure, information on both systolic and diastolic dysfunction is critical in diagnosis, prognosis and guiding therapy.[1] Evaluation of LV function after myocardial infarction provides prognostic information in patient management,[2-4] and guides decision making regarding intervention in patients with valvular heart disease.

Although echocardiography is presently the mainstay of *initial* assessment of patients presenting in heart failure and many other cardiac pathologies, cardiovascular magnetic resonance (CMR) by virtue of its multiparametric nature has the potential to be the principal non-invasive imaging modality for both the diagnosis and the prognosis of the patient with new onset heart failure.

Electronic supplementary material The online version of this article (doi:10.1007/s12350-010-9334-z) contains supplementary material, which is available to authorized users.

From the Department of Cardiology,[a] Flinders Medical Centre, Bedford Park, SA, Australia; and Flinders University,[b] Bedford Park, SA, Australia.

Dr Grover is supported by M and MH Joyner Scholarship in Medicine, Flinders University. Dr Leong is supported by the National Health and Medical Research Council of Australia, the National Heart Foundation of Australia, and the Royal Australasian College of Physicians.

Reprint requests: Joseph B. Selvanayagam, MBBS (Hons), DPhil, Department of Cardiology, Flinders Medical Centre, Bedford Park, SA 5042, Australia; *Joseph.Selvanayagam@flinders.edu.au*.

J Nucl Cardiol 2011;18:351–65.
1071-3581/$34.00

doi:10.1007/s12350-010-9334-z

In this article, we will briefly review the physiology of LV function. We will summarize LV functional assessment using non-nuclear imaging modalities, outlining the role of echocardiography and computed tomography (CT). Our main focus will be on CMR's accurate capacity to assess LV function. Specifically, we will describe the basic principles of CMR image acquisition, and highlight recent advances in image analysis. We will also describe the added advantages of CMR in its ability to characterize tissue; and its role in diastolic function assessment. In addition, the limitations of CMR evaluation of cardiac function will be explored.

MECHANICS OF NORMAL LEFT VENTRICLE FUNCTION

Myocardial performance is dependent on ventricular end-diastolic fiber length (i.e., end-diastolic volume), contractility of the muscle, and the resistance against which contraction occurs. Ejection fraction, used as an overall indicator of myocardial performance, is defined as the ratio of stroke volume to end-diastolic volume. Myocardial fiber stretch, influenced by an increase in end-diastolic volume, leads to more forceful contraction of the cardiac muscle (Frank-Starling mechanism). Similarly, stroke volume may also respond to greater contraction of myocardium, independent of volume, mediated by adrenergic influences. Clearly many factors manipulate these parameters, including pre-loading conditions, myopathies or increases in afterload secondary to hypertension or valvular disease. Heart rate, influencing the duration in which contraction occurs and overall blood volume that has to be pumped provide another complexity for adequate pump function. To appreciate assessment of LV function, it is essential to understand the cardiac ultra structure. Ventricular myocardium, composed of individual striated muscle cells, consists of serially repeating structures (sarcomeres), arranged in rod-like cross-bands (myofibrils). Myocyte structure and arrangement in a helical orientation allows the heart to perform complex 3D motion consisting of radial displacement, rotation, and translation. The characteristic ''wringing motion'' of the heart

described by clockwise rotation of the base, with the anti-clockwise rotation at the apex, allows the heart to develop high intracavitary pressures, with minimal radial displacement.[5] Exactly the opposite motion occurs, just prior to diastole, in which the heart untwists, during isovolumic relaxation. This is an important determinant of elastic recoil and thus diastolic filling and suction. Cardiovascular imaging modalities have the capacity for both reliably measuring these determinants of cardiac function, and in diagnosing the underlying pathology. Through imaging we can explore these interrelationships by measuring volumes, mass, velocities, and perform visual assessment of function in a longitudinal, radial, and circumferential manner, creating a comprehensive profile of myocardial function.

CARDIOVASCULAR MAGNETIC RESONANCE

CMR is considered the gold standard in the evaluation of volumes, mass, and systolic function of both normal and abnormal left ventricles, owing to its high spatial resolution, excellent signal-to-noise ratio, and its ability to image the heart in a three-dimensional (3D) manner. CMR-based assessment of LV function has both diagnostic and prognostic utility in patient evaluation.[6] During the same scan, information on myocardial fibrosis, viability, perfusion, and valvular function can be ascertained, affording considerable versatility in patient assessment. CMR, is highly superior to 2D echocardiography when examining global LV function[7] and allows for follow-up of patients in a temporal manner without cumulative radiation exposure. Its accuracy and reproducibility in the evaluation of volumes, function, and mass make it the standard of reference for all imaging modalities[8-11]

CARDIOVASCULAR MAGNETIC RESONANCE ASSESSMENT OF LEFT VENTRICULAR SYSTOLIC FUNCTION

CMR Functional Image Acquisition: Physics

Cine images are constructed from segmented raw data that is collected during each cardiac cycle for every cardiac phase. Thus, a raw dataset is acquired over 6-7 heart beats.[12] This information is fused to create an averaged movie of ventricular contraction (see Supplementary materials 1 and 2). CMR acquisitions are performed in the conventional orientation, including 4-chamber (horizontal long axis, HLA), 2-chamber (vertical long axis, VLA), 3-chamber (left ventricle outflow tract, LVOT view), and a series of short axis slices allowing 3D assessment of volume and mass.

Early CMR cine sequences were derived from spoiled-gradient echo fast low-angle shot (FLASH) imaging. FLASH sequences rely on inflow enhancement[12,13] to generate blood-myocardial contrast and hence is subject to low contrast-to-noise ratio (CNR), particularly at short repetition times (TR) and low flow rates.[14] This technique has been superseded by a technique that utilizes a short TR time while still delivering high blood to myocardial contrast, allowing for higher in-plane resolution, shorter acquisition times, and better overall image quality.[14,15] Steady state free precession (SSFP) imaging, dependent on a steady state signal based on T2 to T1 ratio has become the cornerstone of cine CMR imaging. It is associated with improved delineation of trabeculae, papillary muscles, the atrioventricular groove, and semi-lunar valves.[15]

There are systematic differences between SSFP and older gradient echo sequences that have been well-documented in head-to-head studies.[16,17] SSFP sequences tend to yield higher end diastolic volume (EDV) and end systolic (ESV) and lower mass.[15,16,18-24] They also allow for greater blood to myocardium and myocardium to fat contrast,[14,15] improving automated contour delineation.[16,19] Use of parallel imaging acquisition techniques have improved scan times, without significantly compromising the spatial and temporal resolutions.[25] The two most common partial parallel acquisition methods utilized are sensitivity encoding (SENSE) and GeneRalized Autocalibrating Partially Parallel Acquisitions (GRAPPA). SENSE provides optimized reconstruction when an accurate coil sensitivity map can be obtained,[26] however, GRAPPA is more lenient when this cannot occur and during patient motion which can lead to significant errors in sensitivity maps.[27]

CMR Functional Image Acquisition: Practical Aspects

The following method is employed at the authors' institution, and is a widely accepted approach to quantify left ventricular (LV) volumes, mass, and function. The methods described may not be possible from all scanner manufacturers, and variations from the described protocol may be necessary. After careful preparation of the patient and explanation of the importance of consistent breath-hold technique, multislice, multi-planar localizer images are performed in a single breath-hold. Prescribing a plane from the transverse plane using the mitral valve and the apex of the left ventricle as anatomical markers, localizer (''pilot'') images are obtained in the vertical long axis (VLA) (Figure 1).

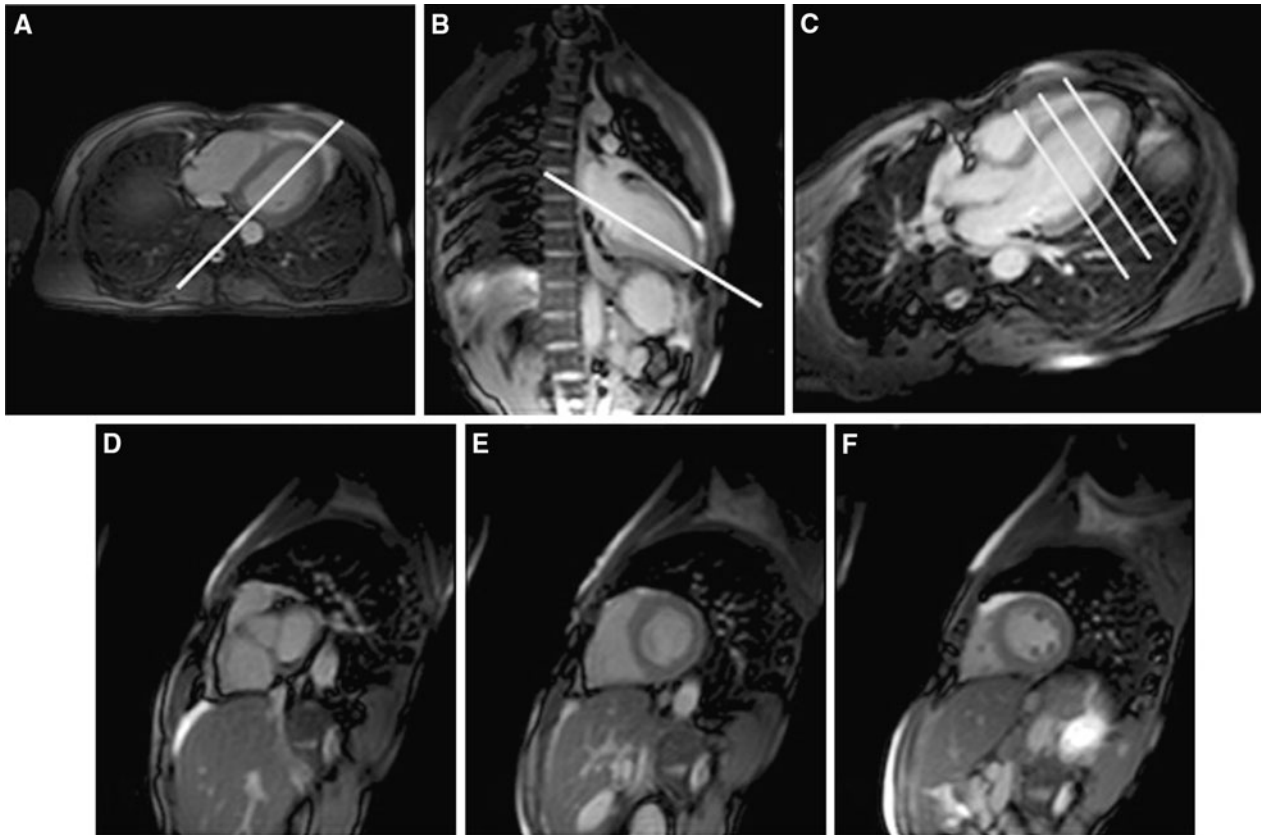

Figure 1. Sequence of images demonstrating the correct acquisition of the long axis and short axis planes for cine imaging. Initially, multi-planar transverse localizer (**A**), in the plane indicated by the *solid line* in (**A**), pilot images are then performed in the vertical long axis (VLA) plane (**B**). The resultant VLA pilot is used to prescribe (as indicated by the *solid line* in **B**) the horizontal long axis (HLA) pilot (**C**). Uing the HLA and VLA pilots, three short axis (SA) slices (**D**-**F**) are next acquired with the basal slice parallel to the atrio-ventricular (AV) groove (indicated by 3 *solid lines* in **C**). Adapted from Selvanayagam et al Cardiovascular Magnetic Resonance—Basic Principles, Methods and Techniques in Hybrid cardiovascular Imaging Dilazian and Pohost (Eds) 2005 Blackwells Scientific Publications.

The resultant VLA pilot is then used to prescribe the horizontal long axis (HLA) pilot using the same anatomical landmarks (Figure 2).

It is important to accurately define the base of the heart when using this or a similar piloting method. As illustrated in Figure 3, using the HLA and VLA pilots, three short axis (SA) slices are acquired with the basal slice parallel to the atrio-ventricular (AV) groove. The distance between the slices is chosen such that they encompass the basal, mid, and apical regions of the ventricle. These ''scout'' images can then be used to plan cine images in two long-axis (HLA and VLA), and left ventricular outflow tract (LVOT) views.

When acquiring the short axis volume stack from the two long axis cines, the position of the basal slice is critical. Most errors in volume calculation are introduced here if this stage is not carefully planned. Using the end-diastolic frames from the VLA and HLA cines, the first slice is placed in the atrio-ventricular (AV) groove. Subsequent slices are placed parallel to this covering the entire ventricle. Typically slice thickness is 7-8 mm with a 3 or 2 mm inter-slice gap. Imaging is usually performed in expiration as this generally produces a more consistent, reproducible breath-hold position.

CMR Functional Data Analysis

Although traditionally considered the Achilles heel of CMR (being both time and labor intensive), there has been major recent advances in automated/semi-automated LV functional assessment, mainly through advances in software development. Currently, quantification of LV functional data is performed off-line using either the MRI vendor provided software platform or a variety of third party software packages (Q MASS,

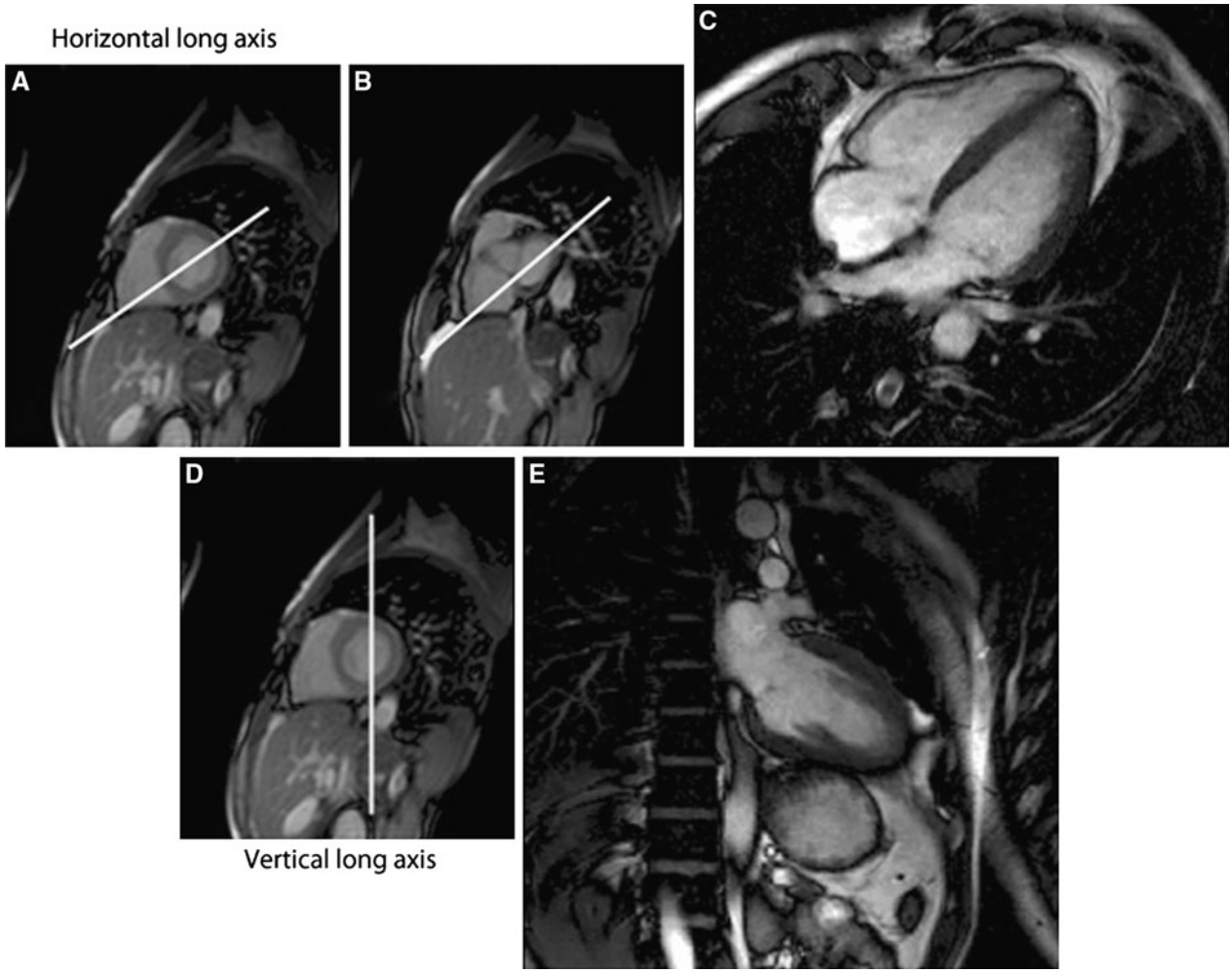

Figure 2. To acquire HLA cine (**C**) the mid ventricular SA pilot (**A**) is used to position the slice through the maximum lateral dimensions of both ventricles and avoid the LVOT as illustrated by panels (**A**) and (**B**). To acquire the VLA cine (**E**), the mid ventricular SA pilot is again used and placed in the plane as indicated in panel (**D**). Adapted from Selvanayagam et al Cardiovascular Magnetic Resonance—Basic Principles, Methods and Techniques in Hybrid cardiovascular Imaging Dilazian and Pohost (Eds) 2005 Blackwells Scientific Publications.

MEDIS Medical Imaging; CAAS MRV, PIE medical imaging; and cmr42, Circle Cardiovascular Imaging) that can be installed on all major computer operating systems. The latter usually provide full DICOM connectivity and therefore can be used as a stand-alone solution, integrated into existing network environments including major Picture Archiving and Communication Systems (PACS).

The LV and RV analyses begin by defining the end-diastolic phase (EDP). Using a mid-ventricular slice, the phases are advanced until the smallest cavity size is reached by visual estimate. This phase is marked as the end-systolic phase (ESP). Most software programs require identification of the EDP, ESP, base, and apex so that the endocardial border can be automatically tracked and volumes calculated (Figure 4).

The greatest sources of variability in the measurement of LV volumes should be acknowledged. The selection of the most basal slice represents the most common error when LV volumes are assessed.[28] By convention the most basal slice is defined as the one where 50% of the slice circumference comprises myocardium. Other sources of error include contour definition and inexperienced operators although the variability induced by the latter can be reduced by a short period of intensive training involving standardized data acquisition, simulated off-line analysis and mentoring.[29]

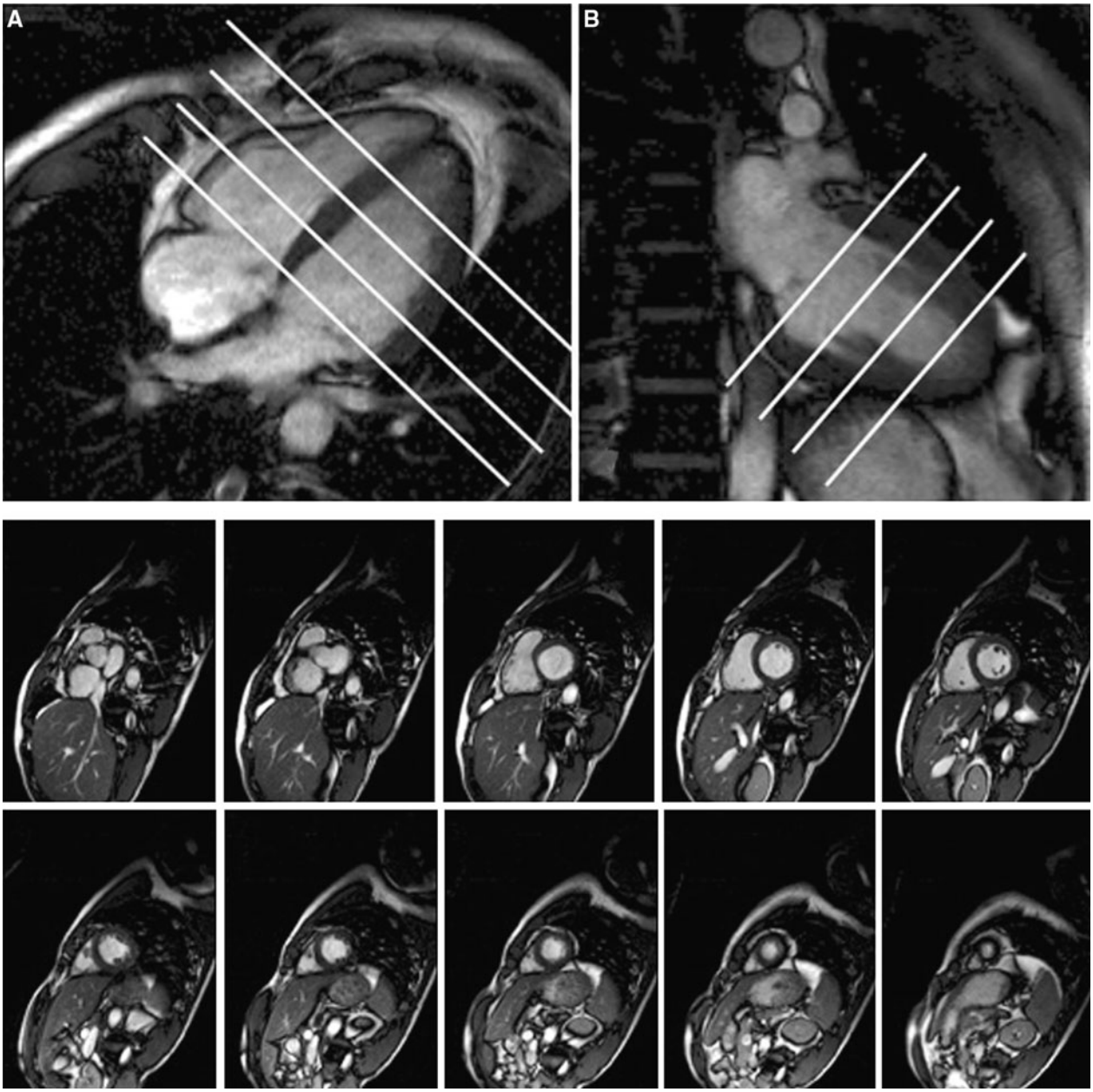

Figure 3. This demonstrates the resultant HLA (**A**), VLA (**B**) and short axis cine stack from base to apex (*bottom panel*). Adapted from Selvanayagam et al Cardiovascular Magnetic Resonance—Basic Principles, Methods and Techniques in Hybrid cardiovascular Imaging Dilazian and Pohost (Eds) 2005 Blackwells Scientific Publications.

REAL-TIME CINE IMAGING

Riederer et al[30] first demonstrated the feasibility of real-time MR imaging in the late eighties. Initial acquisition times were around 250 ms and the predominant interest was in MR fluoroscopy. The evolution of ultrafast imaging sequences such as echo planar imaging[31] and spiral imaging[32] as compared to the more traditional method of accumulating slices of data for a particular image over several cardiac cycles allowed for significant advances in this technique. Data was acquired in short durations leading to images with minimal impact of motion related artifacts. Initial comparative studies found good correlation with conventional imaging sequences in qualitative assessment of LV function and segmental wall thickening,[33] and further quantitative studies showed good agreement with

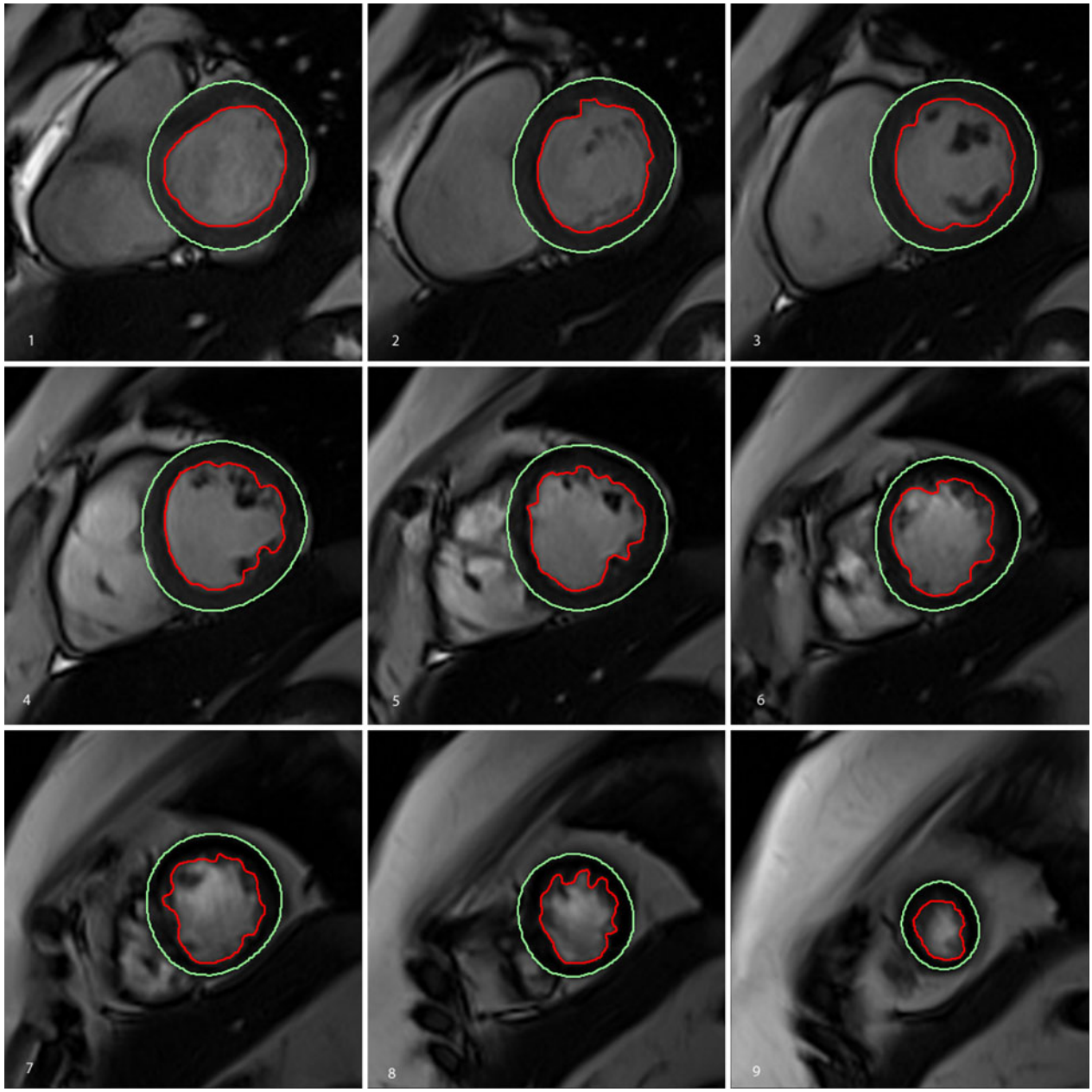

Figure 4. Short axis left ventricular (LV) stack, showing semi-automated contour detection in the end-diastolic phase. Endocardial (*red*) and epicardial (*green*) borders are tracked throughout the series allowing quantitation of LV mass and volume.

the inter and intraobserver variability ranging in the order of 1.9%-10%.[9,18,34-38]

In addition to the ultrafast imaging techniques, advances in real-time reconstruction and display as well as interactive user interface allowed for improved images, particularly used for intracoronary arteries.[39] The use of multiple coils, with real time reconstruction and interactive scanning as allowed current ''real'' time imaging to become a robust tool for assessment of cardiac function. Kuhl et al[40] compared two validated real-time techniques with harmonic 2D imaging, suggesting superiority of radial technique over spiral gradient-echo, achieving similar results to breath-hold SSFP sequence.

Thus far, all the imaging protocols have concentrated on 2D cine imaging, which has been shown to be accurate when assessing cardiac anatomy and function.[41] This usually requires multiple breath-holds, or in

case of real time imaging, does come at the cost of reduced spatial resolution, and image quality. Significant operator expertise is needed in planning the imaging, with some knowledge of cardiac anatomy and pathophysiology essential. Some of these concerns can be overcome using recently described isotropic non-angulated 3D cardiac MR which can be reformatted in any plane, and requires minimal planning.[42,43] Parallel imaging[26,27] and other under sampling techniques[44] have allowed for 3D cine data to be acquired in a single breath-hold.[45-48] The concept of 3D whole heart imaging is not new; static images in 3D were acquired using navigator beams,[49] however, the constant interruptions during the acquisition do not combine well with SSFP cines.[50] Respiratory self-gating which had been used for a variety of 2D and 3D sequences[51-53] was incorporated by Uribe et al to create a ''whole heart 3D acquisition'' addressing the limitations of navigators as well as restricting the duration of the scans.[54] This was performed using a retrospectively ECG gated, balanced SSFP k-space segmented sequence using a five-element cardiac coil array which speeded up the acquisition by applying SENSE.

Recent Advances in Real-Time and 3D Imaging

Although scan times were improved with parallel imaging techniques, often a cost was involved in image degradation using GRAPPA and SENSE at high acceleration factors. The transformation from simple unitary (Fourier) to linear algorithms, to now, use of non-linear algorithms for auto-calibrated parallel imaging, has allowed for significant advancement in speeds of MRI scans. Non-linear algorithms are based on combining variable density trajectories with the joint estimation of image content and coil sensitivities.[55,56] Uecker et al[57] exploited these concepts to perform feasibility of this application for real-time imaging, producing images at frame rates of 20 Hz.

Although the concept of FLASH technique[58] and radial sampling[59] have been around for a considerable time, it is their modified use with repetitive image reconstruction and non-linear inversion that now permits us to produce real-time cine CMR with the correct balance of the spatial and temporal resolutions. Advances in temporal regularization and filtering have led to improvements in data under sampling, in turn, allowing images to be produced at spatial resolutions of 1 to 2 mm in acquisition times of 20 to 30 ms[60,61] in normal subjects. Studies are currently underway to validate this against standard breath-hold 2D image acquisition in a number of cardiac diseased states.

3T IMAGING

High-field imaging has increased signal to noise ratio (SNR) due to increased magnetization of nuclear spins and higher resonance frequency. The increased SNR allows for improvement in spatial/temporal resolution particularly when combined with parallel imaging techniques. It also leads to increased artifact-to-noise ratio, especially with cardiovascular imaging. In early work performed using 3T, Gutberlet et al[62] showed that the increased SNR and contrast-to-noise (CNR) translated to significantly improved anatomical, functional, tagging, phase contrast flow, perfusion, and coronary artery imaging. However, imaging at 3T does require special considerations, limiting its widespread use as a cardiac modality. Almost all implanted devices are considered safe at 1.5T, the same does not hold true for 3T. Specific safety concerns relate to magnetically induced displacement and torque, radiofrequency (RF) heating and image artifact. SSFP imaging used to perform majority of the functional and anatomical image acquisition are especially susceptible to field inhomogenity at 3T. Frequency mismatches lead to signal loss, banding and pulsatility artifacts which can to some extent be addressed localized shimming[63] and frequency scout images.[64] In essence the superior image contrast and SNR at 3T is counteracted by off-resonance artifacts, reduced T2 to T1 ratio leading to longer repetition times and therefore prolonged duration of scan for LV functional assessment.

CMR ASSESSMENT OF DIASTOLIC FUNCTION

Diastolic LV dysfunction is a frequent finding even in the general community.[65] Among patients with organic heart disease, evaluation of diastolic function confers important prognostic value[66] and incremental prognostic information to systolic function.[67] In patients with congestive heart failure, severe diastolic dysfunction has been reported as a potent predictor of cardiac death.[68]

In contrast to the preponderance of studies using CMR to evaluate systolic LV function, assessment of diastolic function using this modality is an emerging field. There are several CMR approaches to characterizing LV filling patterns. First, peak LV filling rates during diastole can be measured by rates of change in chamber volume. Analogous to mitral E/A ratio as assessed by Doppler imaging, volume-derived indices such as peak and early LV filling rate and time to peak early LV filling, are considered sensitive markers of LV diastolic function.[69] At the present time, this approach is limited by the time-consuming nature (even using semi-automated border detection techniques) of the analysis required, and by the relatively low temporal resolution

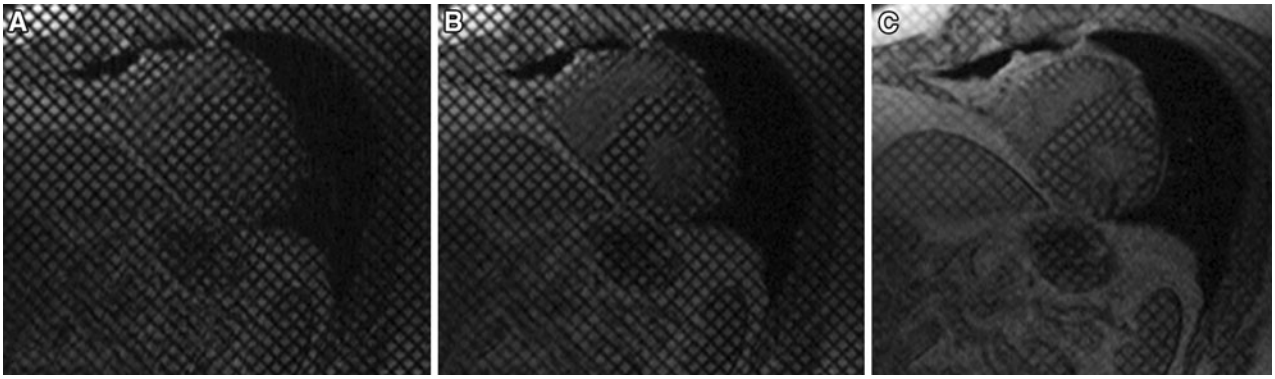

Figure 5. Cardiac tagging short axis images obtained in a normal heart using a complementary spatial modulation of magnetization (CSPAMM) technique. The initial rectangular tagging grid at enddiastole (**A**) is distorted by cardiac contraction, as seen in mid-systole (**B**) and end-systolic image (**C**).

of cine CMR imaging. A second CMR approach for the evaluation of LV filling patterns involves phase-contrast imaging of trans-mitral blood flow for the direct measurement of flow velocity. This method has demonstrated moderate correlation with echocardiography.[70,71] By extension, phase-contrast imaging can be used to measure myocardial tissue velocity. In a comparative study with echocardiographic E/E' and invasive pulmonary capillary wedge pressure, Paelinck et al[72] demonstrated the feasibility of phase-contrast-derived CMR E/E'. The use of this approach has also been restricted by the analysis time required. Recently, Bollache et al[73] have reported on a semi-automated method for the measurement of diastolic parameters. The development of more rapid post-processing software may allow for translation of CMR diastolic evaluation into mainstream clinical practice.

In general, velocities measured by CMR tend to be lower than by echocardiography as a consequence of the lower temporal resolution of CMR. Temporal resolution may be improved by reducing number of views/segment, however, this requires longer breath-hold times.

Myocardial Tagging

The concept of ''tagging'' to quantify regional myocardial function was introduced in 1988, by Zerhouni et al.[74] Tagging involves the labeling of the LV myocardium with radial dark bands in planes perpendicular to the imaging plane. The ''tagged'' grid deforms as the saturated myocardium moves through the cardiac cycle allowing visualization and quantification of regional strain (Figure 5). The tag is generally applied at the onset of the R wave, fading during the cardiac cycle as the magnetization recovers toward equilibrium due to spin lattice relaxation. Although still considered predominantly a research tool, myocardial tagging has been used to demonstrate abnormalities in LV untwisting in aortic stenosis.[75] In a CMR study on the MESA cohort, Edvardsen et al[76] demonstrated that regional diastolic strain rates were significantly reduced in asymptomatic individuals with LV hypertrophy when compared to those without LV hypertrophy.

A key limitation in the use of grid tagging in practice is the tendency of myocardial tags to fade as the cardiac cycle progresses. Early diastolic strain rate was successfully measured in 80% of a relatively normal cohort, however, in the same population atrial tagging was successfully read in only 32%.[76] Comparison at different magnetic fields have shown improved results at 3T.[77] Another limitation in tagging approaches is their failure to account for 3D myocardial deformation (i.e., in- and through-plane). Furthermore, tagging measurement of strain is restricted in spatial resolution by the separation of the tag lines. Lastly, analysis of strain from the tagged dataset has limited availability on commercial CMR analysis software.

Other CMR Approaches to the Assessment of Diastolic LV Function

Velocity-encoded CMR or tissue-phase mapping can evaluate regional systolic and diastolic tissue velocities, in a similar manner to echocardiography.[78,79] Tissue phase mapping technique determines with pixel by pixel resolution velocity tensors in a 3D manner (i.e., rotation, longitudinal, and radial).[80] This has been validated in a non-breath-hold navigator sequence in patients and volunteers. Displacement-encoded imaging using stimulated echoes (DENSE) MRI can also provide a comprehensive assessment of myocardial mechanics

including strain, twist angle, and torsion in an acceptable scan time.[81]

ANCILLARY INFORMATION PROVIDED BY CMR

CMR, in addition to its ability to assess LV and RV function, provides ancillary information that assists in the comprehensive work-up of the patient with cardiac dysfunction. Visual inspection of the left ventricular (LV) and right ventricular (RV) architecture identifies patterns of regional or diffuse wall thinning and concentric or asymmetric hypertrophy,[82] and provide clues to other myopathic processes such as left ventricular non-compaction.[83] Pericardial thickness and calcification can be assessed. The atria and cardiac valves are evaluated for primary or secondary structural abnormalities, and the functional consequences of these morphologic changes are simultaneously evaluated through looped playback of the segmented cine image, making note of regional and global systolic function and valvular flow abnormalities. By providing high-resolution, 3D images, CMR can provide ancillary information on the geometry of the LV, and the presence of mitral regurgitation, or LV thrombus (Figure 6).

Although a detailed discussion is outside the scope of this article, CMR provides unprecedented capability for in vivo myocardial tissue characterization. The development of the late gadolinium enhancement CMR technique (LGE-CMR)[84] has revolutionised the role of cardiovascular magnetic resonance in clinical and research practice, and has potential roles in both diagnosis and prognosis of newly diagnosed heart failure patients. Specific patterns of fibrosis and scarring have been identified in many of the cardiomyopathy states.[85-88] Ischemic cardiomyopathy is characterized by subendocardial-based areas of late enhancement that correlate to irreversible myocardial necrosis on histopathology (Figure 7, 8). Patients who have non-ischemic dilated cardiomyopathy may also have DE-MRI evidence of scarring in up to 30% of cases (Figure 9); however, this is typically in a non-coronary distribution and frequently appears as a mid-wall striae.[87] Diffuse myocardial fibrosis is a final end point in most cardiac diseases and it is missed by the late gadolinium enhancement technique. The calculation of a post-contrast myocardial T1-time following imaging a given plane with sequentially increasing inversion times has recently been shown to discriminate heart failure patients from healthy controls even after excluding myocardial segments displaying late gadolinium enhancement. This technique shows promise in more sensitive and quantitative evaluation of myocardial fibrosis.[89] Flett et al[90] recently demonstrated that an alternative approach of a bolus of extracellular gadolinium contrast followed by continuous infusion to achieve equilibrium together with measurement of T1 time pre- and post-contrast also permits non-invasive quantification of diffuse myocardial fibrosis.

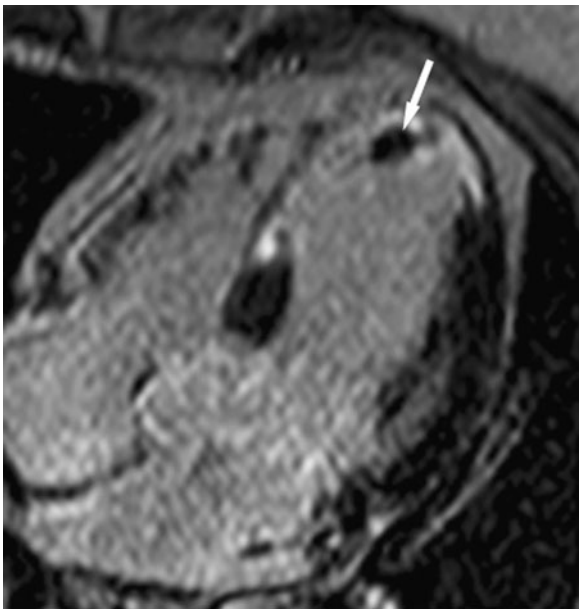

Figure 6. Horizontal long axis (HLA), showing avascular filling defect (*white arrow*) surrounded by transmural hyperenhancement with late gadolinium imaging, consistent with left ventricular thrombus.

LIMITATIONS OF CMR

Most tertiary institutions have access to CMR, however, availability of technical and physician expertise is more limited. This together with cost and slow scanning times are the major limitations of CMR today, although advances in real-time imaging holds promise in over-coming the latter. Standard contraindications including claustrophobia, implanted devices, and other ferromagnetic objects exclude certain populations from undergoing CMR. Gadolinium imaging provides considerable ancillary information in CMR, and its limited use in patients with moderate and severe end-stage renal failure, adds another restriction on widespread use of CMR. Cardiac imaging in particular requires patient co-operation, and careful consideration should be given to the selection of patients undergoing a scan. Questions regarding hearing impairment and breath-holding need to be addressed by the physicians requesting the scan.

TRANSTHORACIC ECHOCARDIOGRAPHY

Echocardiography is the most widely utilized cardiac imaging modality. This is predominantly due to its

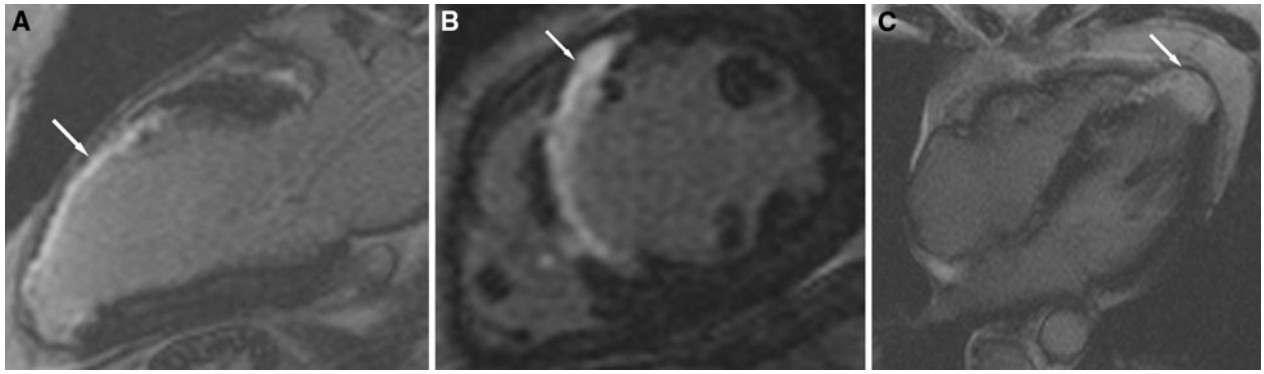

Figure 7. Features of anterior myocardial infarction, with transmural hyperenhancement (*white arrows*) in **A** anterior wall, **B** septum, and **C** apex.

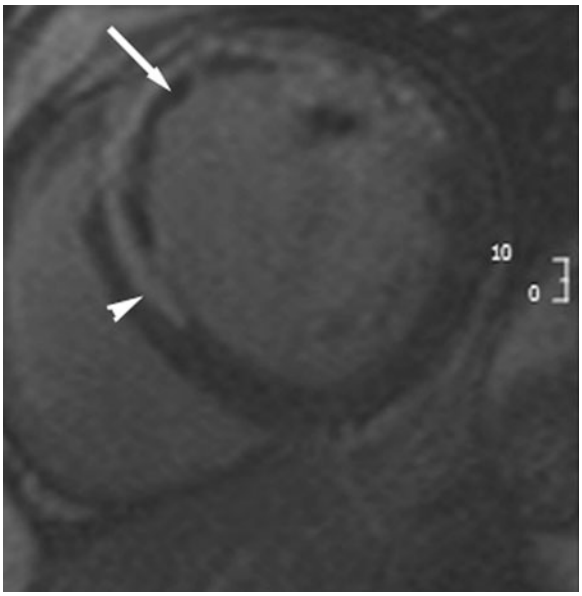

Figure 8. Microvascular obstruction (MVO) characterized by hypoenhanced region (*white arrow*), surrounded by hyperenhancement (*white arrowhead*) on late gadolinium imaging within the myocardium.

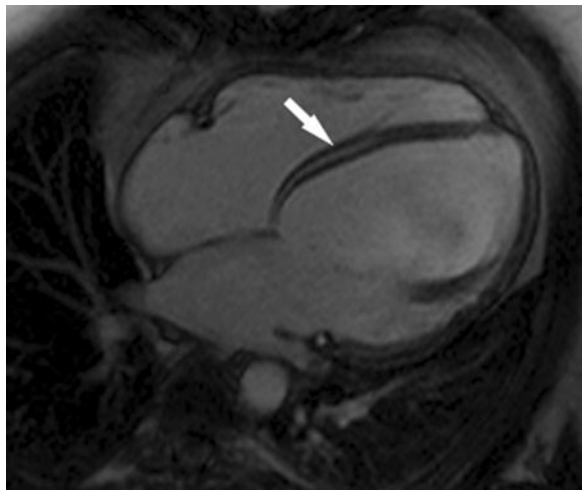

Figure 9. Linear mid-wall hyperenhancement (*white arrow*) within the septum on late gadolinium imaging as is seen in approximately 30% of cases with idiopathic dilated cardiomyopathy.

availability, low-cost, portability, and versatility. However, image quality is heavily dependent of the operator experience, adequate acoustic windows, and geometric assumptions.

Echocardiographic Assessment of LV Systolic Function

The method of choice for 2D assessment of LV function uses the modified Simpsons rule to estimate LV volumes and hence calculate ejection fraction (EF).[91] This technique has well-recognized prognostic value, in a wide number of cardiac disease states.[92-94] Nonetheless Simpson's bi-plane EF suffers from limitations including reliance on endocardial definition, foreshortening of imaging planes and non-uniform chamber geometry. Although 3D echocardiography has circumvented the latter two limitations, it is still subject to greater intermeasurement variability when compared to CMR and computed tomography.[95] Sub-optimal spatial resolution and sub-endocardial definition may occur in up to 20% of patients.[96]

Owing to recognition of the aforementioned limitations, assessment of LV function by echocardiography has undergone significant recent advancement. The use of 3D echocardiography and contrast agents for LV opacification has greatly improved the accuracy of LV assessment by echocardiography. Particularly in patients with difficult acoustic windows, tissue Doppler imaging (TDI) may play a role in aiding diagnosis. Peak tissue velocity at the septal mitral annulus (Sm) represents an integration of longitudinal cardiac motion from base to

apex, providing a surrogate marker of global LV systolic function and is less influenced by suboptimal image quality than 2D imaging. In a study by Ruan et al, it was reported that Sm < 7 cm/s predicted LVEF of <45% with a sensitivity of 93% and specificity of 87%.[97] Although this technique has proven useful in difficult patients, particularly with chronic obstructive pulmonary disease and intensive care ventilated patients, it is still subject to limitations. Tissue Doppler measurements are dependent on the angle of insonation being parallel with the axis of cardiac motion.[98] This may be a particular hindrance in imaging patients with LV dilatation.

Speckle tracking strain is a novel echocardiographic approach that relies on tracking small myocardial regions of interest based on their unique pattern of ultrasound backscatter. This allows calculation of tissue deformation (strain) on a regional basis and segmental scores can then be averaged to yield a global strain score. Speckle tracking strain, in contrast to tissue Doppler-derived strain, is independent of angle of ultrasound insonation and has been shown to provide additional prognostic information in prediction of adverse cardiac events.[99] Becker et al[100] have demonstrated close agreement between speckle-tracking strain and CMR in the evaluation of regional wall function.

COMPUTED TOMOGRAPHY

Multi-detector computed tomography (MDCT) is principally known for its non-invasive assessment of coronary arteries, although recent developments have enabled it to provide added information on global and regional myocardial function. It is also highly sensitive non-invasive diagnostic modality for determination of coronary calcium as this has high x-ray attenuation, however, data on predictive value of coronary calcium score in addition to the traditional risk factors has been controversial.[101] Current generation 64 slice scanners with improved temporal and spatial resolution provide excellent visualization of the proximal and distal coronary vasculature; and have been validated in assessment of LV function with 2D echocardiography and CMR.[102-104] With the improved endocardial definition now available with CT, assessment of LV volumes and ejection fraction are routinely possible. Differences in intermodality acquisition methods and analysis strategy are thought responsible for the tendency of CT to overestimate volumes and underestimate EF as compared to CMR.[105-107] Although cardiac CT may well play an increasingly important role in providing anatomical and functional information, it has limited utility in tissue characterization and exposes patients to ionizing radiation: CMR overcomes both these limitations.

CONCLUSION

CMR is often described as the ''one stop shop'' for evaluating cardiac diseases. It is a 3D imaging technique that affords unprecedented spatial resolution, ability to interogate any imaging plane and consistently high image quality. Evaluation of LV function is of key importance in categorizing patient pathology. In addition to its role in functional assessment, CMR provides information on flow, perfusion, diastology, and tissue characterization, often alleviating the need for invasive procedures. It does require patient co-operation with breath-holds and tolerability of the scan. A standard volume assessment can be performed in 10 minutes in a typical clinical environment; however, scans often require additional information on flows, viability, stress, leading to a typical acquisition time of 35 to 45 minutes. This is considered to be the greatest limitation of cardiac MRI. With real-time imaging, now becoming more than just a research tool, as well as 3D acquisition of data sets in single breath-hold, without compromising spatial resolution, CMR is becoming time efficient. The comprehensive nature of a CMR assessment is well-known, and now with increased speed of acquisition and hence decrease in the scan times will truly make CMR imaging the first line imaging modality for cardiac assessment.

Conflicts of interest

The authors have indicated that they have no financial conflicts of interest.

References

1. Hunt SA, Baker DW, Chin MH, Cinquegrani MP, Feldman AM, Francis GS, et al. ACC/AHA guidelines for the evaluation and management of chronic heart failure in the adult: Executive summary. J Heart Lung Transplant 2002;21:189-203.
2. Schwammenthal E, Adler Y, Amichai K, Sagie A, Behar S, Hod H, et al. Prognostic value of global myocardial performance indices in acute myocardial infarction: Comparison to measures of systolic and diastolic left ventricular function. Chest 2003;124:1645-51.
3. Braunwald E, Antman EM, Beasley JW, Califf RM, Cheitlin MD, Hochman JS, et al. ACC/AHA 2002 guideline update for the management of patients with unstable angina and non-ST-segment elevation myocardial infarction-summary article: A report of the American College of Cardiology/American Heart Association task force on practice guidelines (Committee on the Management of Patients With Unstable Angina). J Am Coll Cardiol 2002;40:1366-74.
4. Ryan TJ, Antman EM, Brooks NH, Califf RM, Hillis LD, Hiratzka LF, et al. 1999 update: ACC/AHA guidelines for the management of patients with acute myocardial infarction. A report of the American College of Cardiology/American Heart Association Task Force on Practice Guidelines (Committee on

Management of Acute Myocardial Infarction). J Am Coll Cardiol 1999;34:890-911.
5. Nagel E, Stuber M, Fleck E, Boesiger P, Hess OM. Myocardial tagging for the analysis left ventricular function. MAGMA 1998;6:91-3.
6. Hundley WG, Morgan TM, Neagle CM, Hamilton CA, Rerkpattanapipat P, Link KM. Magnetic resonance imaging determination of cardiac prognosis. Circulation 2002;106:2328-33.
7. Bellenger NG, Burgess MI, Ray SG, Lahiri A, Coats AJ, Cleland JG, et al. Comparison of left ventricular ejection fraction and volumes in heart failure by echocardiography, radionuclide ventriculography and cardiovascular magnetic resonance; are they interchangeable? Eur Heart J 2000;21:1387-96.
8. Debatin JF, Nadel SN, Paolini JF, Sostman HD, Coleman RE, Evans AJ, et al. Cardiac ejection fraction: Phantom study comparing cine MR imaging, radionuclide blood pool imaging, and ventriculography. J Magn Reson Imaging 1992;2:135-42.
9. Sakuma H, Fujita N, Foo TK, Caputo GR, Nelson SJ, Hartiala J, et al. Evaluation of left ventricular volume and mass with breath-hold cine MR imaging. Radiology 1993;188:377-80.
10. Bellenger NG, Davies LC, Francis JM, Coats AJ, Pennell DJ. Reduction in sample size for studies of remodeling in heart failure by the use of cardiovascular magnetic resonance. J Cardiovasc Magn Reson 2000;2:271-8.
11. Wintersperger BJ, Nikolaou K, Dietrich O, Rieber J, Nittka M, Reiser MF, et al. Single breath-hold real-time cine MR imaging: Improved temporal resolution using generalized autocalibrating partially parallel acquisition (GRAPPA) algorithm. Eur Radiol 2003;13:1931-6.
12. Atkinson DJ, Edelman RR. Cineangiography of the heart in a single breath hold with a segmented turboFLASH sequence. Radiology 1991;178:357-60.
13. Foo TK, Bernstein MA, Aisen AM, Hernandez RJ, Collick BD, Bernstein T. Improved ejection fraction and flow velocity estimates with use of view sharing and uniform repetition time excitation with fast cardiac techniques. Radiology 1995; 195:471-8.
14. Carr JC, Simonetti O, Bundy J, Li D, Pereles S, Finn JP. Cine MR angiography of the heart with segmented true fast imaging with steady-state precession. Radiology 2001;219:828-34.
15. Moon JC, Lorenz CH, Francis JM, Smith GC, Pennell DJ. Breath-hold FLASH and FISP cardiovascular MR imaging: Left ventricular volume differences and reproducibility. Radiology 2002;223:789-97.
16. Plein S, Bloomer TN, Ridgway JP, Jones TR, Bainbridge GJ, Sivananthan MU. Steady-state free precession magnetic resonance imaging of the heart: Comparison with segmented k-space gradient-echo imaging. J Magn Reson Imaging 2001;14:230-6.
17. Alfakih K, Thiele H, Plein S, Bainbridge GJ, Ridgway JP, Sivananthan MU. Comparison of right ventricular volume measurement between segmented k-space gradient-echo and steady-state free precession magnetic resonance imaging. J Magn Reson Imaging 2002;16:253-8.
18. Lorenz CH, Walker ES, Morgan VL, Klein SS, Graham TP Jr. Normal human right and left ventricular mass, systolic function, and gender differences by cine magnetic resonance imaging. J Cardiovasc Magn Reson 1999;1:7-21.
19. Barkhausen J, Ruehm SG, Goyen M, Buck T, Laub G, Debatin JF. MR evaluation of ventricular function: True fast imaging with steady-state precession versus fast low-angle shot cine MR imaging: Feasibility study. Radiology 2001;219:264-9.
20. Alfakih K, Plein S, Thiele H, Jones T, Ridgway JP, Sivananthan MU. Normal human left and right ventricular dimensions for MRI as assessed by turbo gradient echo and steady-state free precession imaging sequences. J Magn Reson Imaging 2003;17: 323-9.
21. Marcus JT, DeWaal LK, Gotte MJ, van der Geest RJ, Heethaar RM, Van Rossum AC. MRI-derived left ventricular function parameters and mass in healthy young adults: Relation with gender and body size. Int J Card Imaging 1999;15:411-9.
22. Rominger MB, Bachmann GF, Pabst W, Rau WS. Right ventricular volumes and ejection fraction with fast cine MR imaging in breath-hold technique: Applicability, normal values from 52 volunteers, and evaluation of 325 adult cardiac patients. J Magn Reson Imaging1999;10:908-18.
23. Sandstede J, Lipke C, Beer M, Hofmann S, Pabst T, Kenn W, et al. Age- and gender-specific differences in left and right ventricular cardiac function and mass determined by cine magnetic resonance imaging. Eur Radiol 2000;10:438-42.
24. Li W, Stern JS, Mai VM, Pierchala LN, Edelman RR, Prasad PV. MR assessment of left ventricular function: Quantitative comparison of fast imaging employing steady-state acquisition (FIESTA) with fast gradient echo cine technique. J Magn Reson Imaging 2002;16:559-64.
25. Kunz RP, Oellig F, Krummenauer F, Oberholzer K, Romaneehsen B, Vomweg TW, et al. Assessment of left ventricular function by breath-hold cine MR imaging: Comparison of different steady-state free precession sequences. J Magn Reson Imaging 2005;21:140-8.
26. Pruessmann KP, Weiger M, Scheidegger MB, Boesiger P. SENSE: Sensitivity encoding for fast MRI. Magn Reson Med 1999;42:952-62.
27. Griswold MA, Jakob PM, Heidemann RM, Nittka M, Jellus V, Wang J, et al. Generalized autocalibrating partially parallel acquisitions (GRAPPA). Magn Reson Med 2002;47:1202-10.
28. Marcus JT, Gotte MJ, DeWaal LK, Stam MR, Van der Geest RJ, Heethaar RM, et al. The influence of through-plane motion on left ventricular volumes measured by magnetic resonance imaging: Implications for image acquisition and analysis. J Cardiovasc Magn Reson 1999;1:1-6.
29. Karamitsos TD, Hudsmith LE, Selvanayagam JB, Neubauer S, Francis JM. Operator induced variability in left ventricular measurements with cardiovascular magnetic resonance is improved after training. J Cardiovasc Magn Reson 2007;9:777-83.
30. Riederer SJ, Tasciyan T, Farzaneh F, Lee JN, Wright RC, Herfkens RJ. MR fluoroscopy: Technical feasibility. Magn Reson Med 1988;8:1-15.
31. McKinnon GC. Ultrafast interleaved gradient-echo-planar imaging on a standard scanner. Magn Reson Med 1993;30:609-16.
32. Ahn CB, Kim JH, Cho ZH. High-speed spiral-scan echo planar NMR imaging—I. IEEE Trans Med Imaging 1986;5:2-7.
33. Scheidegger MB, Spiegel M, Stuber M, Bonetti P, Dubach P, Boesiger P. Assessment of cardiac wall thickening and ejection fraction from real time cardiac MR images in patients with left ventricular dysfunction. In: Proceedings ISMRM; 1998. p. 1-554
34. Semelka RC, Tomei E, Wagner S, Mayo J, Kondo C, Suzuki J, et al. Normal left ventricular dimensions and function: Interstudy reproducibility of measurements with cine MR imaging. Radiology 1990;174:763-8.
35. Semelka RC, Tomei E, Wagner S, Mayo J, Caputo G, O'Sullivan M, et al. Interstudy reproducibility of dimensional and functional measurements between cine magnetic resonance studies in the morphologically abnormal left ventricle. Am Heart J 1990;119: 1367-73.
36. Butler SP, McKay E, Paszkowski AL, Quinn RJ, Shnier RC, Donovan JT. Reproducibility study of left ventricular measurements with breath-hold cine MRI using a semiautomated

volumetric image analysis program. J Magn Reson Imaging 1998;8:467-72.
37. Caputo GR, Suzuki J, Kondo C, Cho H, Quaife RA, Higgins CB, et al. Determination of left ventricular volume and mass with use of biphasic spin-echo MR imaging: Comparison with cine MR. Radiology 1990;177:773-7.
38. Plein S, Smith WH, Ridgway JP, Kassner A, Beacock DJ, Bloomer TN, et al. Measurements of left ventricular dimensions using real-time acquisition in cardiac magnetic resonance imaging: Comparison with conventional gradient echo imaging. MAGMA 2001;13:101-8.
39. Hardy CJ, Darrow RD, Pauly JM, Kerr AB, Dumoulin CL, Hu BS, et al. Interactive coronary MRI. Magn Reson Med 1998;40: 105-11.
40. Kuhl HP, Spuentrup E, Wall A, Franke A, Schroder J, Heussen N, et al. Assessment of myocardial function with interactive non-breath-hold real-time MR imaging: Comparison with echocardiography and breath-hold Cine MR imaging. Radiology 2004;231:198-207.
41. Grothues F, Smith GC, Moon JC, Bellenger NG, Collins P, Klein HU, et al. Comparison of interstudy reproducibility of cardiovascular magnetic resonance with two-dimensional echocardiography in normal subjects and in patients with heart failure or left ventricular hypertrophy. Am J Cardiol. 2002;90:29-34.
42. Sorensen TS, Korperich H, Greil GF, Eichhorn J, Barth P, Meyer H, et al. Operator-independent isotropic three-dimensional magnetic resonance imaging for morphology in congenital heart disease: A validation study. Circulation 2004;110:163-9.
43. Razavi RS, Hill DL, Muthurangu V, Miquel ME, Taylor AM, Kozerke S, et al. Three-dimensional magnetic resonance imaging of congenital cardiac anomalies. Cardiol Young 2003;13:461-5.
44. Kozerke S, Tsao J, Pruessmann KP, Boesiger P. Accelerating cardiac cine 3D SSFP imaging using k-t BLAST with integrated training. In: Proceedings of the 11th Annual Meeting of ISMRM, Toronto, Canada; 2003
45. Noble N, Boubertakh R, Muthurangu V, Razavi R, Hill D. A 4D single breath hold cardiac MR examination. In: Proceedings of the 13th Annual Meeting of ISMRM. Miami, USA; 2005
46. Muthurangu V, Noble N, Boubertakh R, Winkelmann R, Johnson R, Bornert P, et al. Single breath-hold 3D cine imaging: A non-angulated isotropic acquisition using SENSE on a 32 channel system. In: Proceedings of 9th annual meeting of SCMR. Miami, USA; 2006
47. Muthurangu V, Noble N, Boubertakh R, Hill D, Razavi R. Assessment of ventricular function and dynamic anatomy using 4D cardiac data acquired in a single breath hold. In: Proceedings of 13th Annual Meeting of ISMRM. Miami, USA; 2005
48. Kellman P, McVeigh ER. Single breath-hold 3D cine cardiac imaging of the entire heart with 32 channel parallel imaging. In: Proceedings of the 13th Annual Meeting of ISMRM. Miami, USA; 2005
49. Pearlman JD, Hardy CJ, Cline HE. Continual NMR cardiography without gating: M-mode MR imaging. Radiology 1990;175:369-73.
50. Scheffler K, Lehnhardt S. Principles and applications of balanced SSFP techniques. Eur Radiol 2003;13:2409-18.
51. Larson AC, Kellman P, Arai A, Hirsch GA, McVeigh E, Li D, et al. Preliminary investigation of respiratory self-gating for free-breathing segmented cine MRI. Magn Reson Med 2005;53: 159-68.
52. Stehning C, Bornert P, Nehrke K, Eggers H, Stuber M. Free-breathing whole-heart coronary MRA with 3D radial SSFP and self-navigated image reconstruction. Magn Reson Med 2005;54:476-80.
53. Hardy CJ, Zhao L, Zong X, Saranathan M, Yucel EK. Coronary MR angiography: Respiratory motion correction with BACSPIN. J Magn Reson Imaging 2003;17:170-6.
54. Uribe S, Muthurangu V, Boubertakh R, Schaeffter T, Razavi R, Hill DL, et al. Whole-heart cine MRI using real-time respiratory self-gating. Magn Reson Med 2007;57:606-13.
55. Ying L, Sheng J. Joint image reconstruction and sensitivity estimation in SENSE (JSENSE). Magn Reson Med 2007;57: 1196-202.
56. Uecker M, Hohage T, Block KT, Frahm J. Image reconstruction by regularized nonlinear inversion-joint estimation of coil sensitivities and image content. Magn Reson Med 2008;60:674-82.
57. Uecker M, Zhang S, Frahm J. Nonlinear inverse reconstruction for real-time MRI of the human heart using undersampled radial FLASH. Magn Reson Med 2010;63:1456-62.
58. Lauterbur PC. Image formation by induced local interactions. Examples employing nuclear magnetic resonance. 1973. Clin Orthop Relat Res 1989;244:3-6.
59. Frahm J, Haase A, Matthaei D. Rapid NMR imaging of dynamic processes using the FLASH technique. Magn Reson Med 1986;3:321-7.
60. Zhang S, Block KT, Frahm J. Magnetic resonance imaging in real time: Advances using radial FLASH. J Magn Reson Imaging 2010;31:101-9.
61. Zhang S, Uecker M, Voit D, Merboldt KD, Frahm J. Real-time cardiovascular magnetic resonance at high temporal resolution: Radial FLASH with nonlinear inverse reconstruction. J Cardiovasc Magn Reson 2010;12:39.
62. Gutberlet M, Noeske R, Schwinge K, Freyhardt P, Felix R, Niendorf T. Comprehensive cardiac magnetic resonance imaging at 3.0 Tesla: Feasibility and implications for clinical applications. Invest Radiol 2006;41:154-67.
63. Schar M, Kozerke S, Fischer SE, Boesiger P. Cardiac SSFP imaging at 3 Tesla. Magn Reson Med 2004;51:799-806.
64. Deshpande VS, Shea SM, Li D. Artifact reduction in true-FISP imaging of the coronary arteries by adjusting imaging frequency. Magn Reson Med 2003;49:803-9.
65. Abhayaratna WP, Marwick TH, Smith WT, Becker NG. Characteristics of left ventricular diastolic dysfunction in the community: An echocardiographic survey. Heart 2006;92: 1259-64.
66. Raunso J, Moller JE, Kjaergaard J, Akkan D, Hassager C, Torp-Pedersen C, et al. Prognostic importance of a restrictive transmitral filling pattern in patients with symptomatic congestive heart failure and atrial fibrillation. Am Heart J 2009;158:983-8.
67. Shanks M, Ng AC, van de Veire NR, Antoni ML, Bertini M, Delgado V, et al. Incremental prognostic value of novel left ventricular diastolic indexes for prediction of clinical outcome in patients with ST-elevation myocardial infarction. Am J Cardiol 2010;105:592-7.
68. Xie GY, Berk MR, Smith MD, Gurley JC, DeMaria AN. Prognostic value of Doppler transmitral flow patterns in patients with congestive heart failure. J Am Coll Cardiol 1994;24:132-9.
69. Kudelka AM, Turner DA, Liebson PR, Macioch JE, Wang JZ, Barron JT. Comparison of cine magnetic resonance imaging and Doppler echocardiography for evaluation of left ventricular diastolic function. Am J Cardiol 1997;80:384-6.
70. Rubinshtein R, Glockner JF, Feng D, Araoz PA, Kirsch J, Syed IS, et al. Comparison of magnetic resonance imaging versus Doppler echocardiography for the evaluation of left ventricular diastolic function in patients with cardiac amyloidosis. Am J Cardiol 2009;103:718-23.
71. Rathi VK, Doyle M, Yamrozik J, Williams RB, Caruppannan K, Truman C, et al. Routine evaluation of left ventricular diastolic

function by cardiovascular magnetic resonance: A practical approach. J Cardiovasc Magn Reson 2008;10:36.
72. Paelinck BP, de Roos A, Bax JJ, Bosmans JM, van Der Geest RJ, Dhondt D, et al. Feasibility of tissue magnetic resonance imaging: A pilot study in comparison with tissue Doppler imaging and invasive measurement. J Am Coll Cardiol 2005;45:1109-16.
73. Bollache E, Redheuil A, Clement-Guinaudeau S, Defrance C, Perdrix L, Ladouceur M, et al. Automated left ventricular diastolic function evaluation from phase-contrast cardiovascular magnetic resonance and comparison with Doppler echocardiography. J Cardiovasc Magn Reson 2010;12:63.
74. Zerhouni EA, Parish DM, Rogers WJ, Yang A, Shapiro EP. Human heart: Tagging with MR imaging-a method for noninvasive assessment of myocardial motion. Radiology 1988;169: 59-63.
75. Nagel E, Stuber M, Burkhard B, Fischer SE, Scheidegger MB, Boesiger P, et al. Cardiac rotation and relaxation in patients with aortic valve stenosis. Eur Heart J 2000;21:582-9.
76. Edvardsen T, Rosen BD, Pan L, Jerosch-Herold M, Lai S, Hundley WG, et al. Regional diastolic dysfunction in individuals with left ventricular hypertrophy measured by tagged magnetic resonance imaging-the Multi-Ethnic Study of Atherosclerosis (MESA). Am Heart J 2006;151:109-14.
77. Valeti VU, Chun W, Potter DD, Araoz PA, McGee KP, Glockner JF, et al. Myocardial tagging and strain analysis at 3 Tesla: Comparison with 1.5 Tesla imaging. J Magn Reson Imaging 2006;23:477-80.
78. Petersen SE, Jung BA, Wiesmann F, Selvanayagam JB, Francis JM, Hennig J, et al. Myocardial tissue phase mapping with cine phase-contrast mr imaging: Regional wall motion analysis in healthy volunteers. Radiology 2006;238:816-26.
79. Jung B, Foll D, Bottler P, Petersen S, Hennig J, Markl M. Detailed analysis of myocardial motion in volunteers and patients using high-temporal-resolution MR tissue phase mapping. J Magn Reson Imaging 2006;24:1033-9.
80. Hennig J, Schneider B, Peschl S, Markl M, Krause T, Laubenberger J. Analysis of myocardial motion based on velocity measurements with a black blood prepared segmented gradient-echo sequence: Methodology and applications to normal volunteers and patients. J Magn Reson Imaging 1998;8:868-77.
81. Gilson WD, Yang Z, French BA, Epstein FH. Measurement of myocardial mechanics in mice before and after infarction using multislice displacement-encoded MRI with 3D motion encoding. Am J Physiol Heart Circ Physiol 2005;288:H1491-7.
82. Rickers C, Wilke NM, Jerosch-Herold M, Casey SA, Panse P, Panse N, et al. Utility of cardiac magnetic resonance imaging in the diagnosis of hypertrophic cardiomyopathy. Circulation 2005;112:855-61.
83. Petersen SE, Selvanayagam JB, Wiesmann F, Robson MD, Francis JM, Anderson RH, et al. Left ventricular non-compaction: Insights from cardiovascular magnetic resonance imaging. J Am Coll Cardiol 2005;46:101-5.
84. Simonetti OP, Kim RJ, Fieno DS, Hillenbrand HB, Wu E, Bundy JM, et al. An improved MR imaging technique for the visualization of myocardial infarction. Radiology 2001;218:215-23.
85. Mahrholdt H, Wagner A, Judd RM, Sechtem U, Kim RJ. Delayed enhancement cardiovascular magnetic resonance assessment of non-ischaemic cardiomyopathies. Eur Heart J 2005;26:1461-74.
86. Moon JC, McKenna WJ, McCrohon JA, Elliott PM, Smith GC, Pennell DJ. Toward clinical risk assessment in hypertrophic cardiomyopathy with gadolinium cardiovascular magnetic resonance. J Am Coll Cardiol 2003;41:1561-7.
87. McCrohon JA, Moon JC, Prasad SK, McKenna WJ, Lorenz CH, Coats AJ, et al. Differentiation of heart failure related to dilated cardiomyopathy and coronary artery disease using gadolinium-enhanced cardiovascular magnetic resonance. Circulation 2003;108:54-9.
88. Moon JCC, Sachdev B, Elkington AG, McKenna WJ, Mehta A, Pennell DJ, et al. Gadolinium enhanced cardiovascular magnetic resonance in Anderson-Fabry disease1: Evidence for a disease specific abnormality of the myocardial interstitium. Eur Heart J 2003;24:2151-5.
89. Iles L, Pfluger H, Phrommintikul A, Cherayath J, Aksit P, Gupta SN, et al. Evaluation of diffuse myocardial fibrosis in heart failure with cardiac magnetic resonance contrast-enhanced T1 mapping. J Am Coll Cardiol 2008;52:1574-80.
90. Flett AS, Hayward MP, Ashworth MT, Hansen MS, Taylor AM, Elliott PM, et al. Equilibrium contrast cardiovascular magnetic resonance for the measurement of diffuse myocardial fibrosis: Preliminary validation in humans. Circulation 2010;122:138-44.
91. Lang RM, Bierig M, Devereux RB, Flachskampf FA, Foster E, Pellikka PA, et al. Recommendations for chamber quantification: A report from the American Society of Echocardiography's Guidelines and Standards Committee and the Chamber Quantification Writing Group, developed in conjunction with the European Association of Echocardiography, a branch of the European Society of Cardiology. J Am Soc Echocardiogr 2005;18:1440-63.
92. Thune JJ, Kober L, Pfeffer MA, Skali H, Anavekar NS, Bourgoun M, et al. Comparison of regional versus global assessment of left ventricular function in patients with left ventricular dysfunction, heart failure, or both after myocardial infarction: The valsartan in acute myocardial infarction echocardiographic study. J Am Soc Echocardiogr 2006;19:1462-5.
93. Cintron G, Johnson G, Francis G, Cobb F, Cohn JN. Prognostic significance of serial changes in left ventricular ejection fraction in patients with congestive heart failure. The V-HeFT VA Cooperative Studies Group. Circulation 1993;87:VI17-23.
94. St John Sutton M, Otterstat JE, Plappert T, Parker A, Sekarski D, Keane MG, et al. Quantitation of left ventricular volumes and ejection fraction in post-infarction patients from biplane and single plane two-dimensional echocardiograms. A prospective longitudinal study of 371 patients. Eur Heart J 1998;19:808-16.
95. Sugeng L, Mor-Avi V, Weinert L, Niel J, Ebner C, Steringer-Mascherbauer R, et al. Quantitative assessment of left ventricular size and function: Side-by-side comparison of real-time three-dimensional echocardiography and computed tomography with magnetic resonance reference. Circulation 2006;114:654-61.
96. Tighe DA, Rosetti M, Vinch CS, Chandok D, Muldoon D, Wiggin B, et al. Influence of image quality on the accuracy of real time three-dimensional echocardiography to measure left ventricular volumes in unselected patients: A comparison with gated-SPECT imaging. Echocardiography 2007;24:1073-80.
97. Ruan Q, Nagueh SF. Usefulness of isovolumic and systolic ejection signals by tissue Doppler for the assessment of left ventricular systolic function in ischemic or idiopathic dilated cardiomyopathy. Am J Cardiol 2006;97:872-5.
98. Urheim S, Edvardsen T, Torp H, Angelsen B, Smiseth OA. Myocardial strain by Doppler echocardiography. Validation of a new method to quantify regional myocardial function. Circulation 2000;102:1158-64.
99. Cho GY, Marwick TH, Kim HS, Kim MK, Hong KS, Oh DJ. Global 2-dimensional strain as a new prognosticator in patients with heart failure. J Am Coll Cardiol 2009;54:618-24.
100. Becker M, Hoffmann R, Kuhl HP, Grawe H, Katoh M, Kramann R, et al. Analysis of myocardial deformation based on ultrasonic pixel tracking to determine transmurality in chronic myocardial infarction. Eur Heart J 2006;27:2560-6.

101. O'Rourke RA, Brundage BH, Froelicher VF, Greenland P, Grundy SM, Hachamovitch R, et al. American College of Cardiology/American Heart Association Expert Consensus document on electron-beam computed tomography for the diagnosis and prognosis of coronary artery disease. Circulation 2000;102:126-40.
102. Salm LP, Schuijf JD, de Roos A, Lamb HJ, Vliegen HW, Jukema JW, et al. Global and regional left ventricular function assessment with 16-detector row CT: Comparison with echocardiography and cardiovascular magnetic resonance. Eur J Echocardiogr 2006;7:308-14.
103. Ko SM, Kim YJ, Park JH, Choi NM. Assessment of left ventricular ejection fraction and regional wall motion with 64-slice multidetector CT: A comparison with two-dimensional transthoracic echocardiography. Br J Radiol 2010;83:28-34.
104. van der Vleuten PA, Willems TP, Gotte MJ, Tio RA, Greuter MJ, Zijlstra F, et al. Quantification of global left ventricular function: Comparison of multidetector computed tomography and magnetic resonance imaging. A meta-analysis and review of the current literature. Acta Radiol 2006;47:1049-57.
105. Grude M, Juergens KU, Wichter T, Paul M, Fallenberg EM, Muller JG, et al. Evaluation of global left ventricular myocardial function with electrocardiogram-gated multidetector computed tomography: Comparison with magnetic resonance imaging. Invest Radiol 2003;38:653-61.
106. Juergens KU, Grude M, Maintz D, Fallenberg EM, Wichter T, Heindel W, et al. Multi-detector row CT of left ventricular function with dedicated analysis software versus MR imaging: Initial experience. Radiology 2004;230:403-10.
107. Mahnken AH, Katoh M, Bruners P, Spuentrup E, Wildberger JE, Gunther RW, et al. Acute myocardial infarction: Assessment of left ventricular function with 16-detector row spiral CT versus MR imaging—study in pigs. Radiology 2005;236:112-7.